Nanostructures of zinc oxide

by Zhong Lin Wang

Zinc oxide (ZnO) is a unique material that exhibits semiconducting, piezoelectric, and pyroelectric multiple properties. Using a solid-vapor phase thermal sublimation technique, nanocombs, nanorings, nanohelixes/nanosprings, nanobows, nanobelts, nanowires, and nanocages of ZnO have been synthesized under specific growth conditions. These unique nanostructures unambiguously demonstrate that ZnO is probably the richest family of nanostructures among all materials, both in structures and properties. The nanostructures could have novel applications in optoelectronics, sensors, transducers, and biomedical science because it is bio-safe.

School of Materials Science and Engineering,
Georgia Institute of Technology,
Atlanta, GA 30332-0245 USA
E-mail: zhong.wang@mse.gatech.edu

Since the discovery of oxide nanobelts of semiconducting oxides in 2001[1], research into functional oxide-based, one-dimensional nanostructures has rapidly expanded because of their unique and novel applications in optics, optoelectronics, catalysis, and piezoelectricity. Semiconducting oxide nanobelts are a unique group of quasi-one-dimensional nanomaterials, which have been systematically studied for a wide range of materials with distinct chemical compositions and crystallographic structures.

Belt-like, quasi-one-dimensional nanostructures (called nanobelts) have been synthesized for semiconducting oxides of Zn, Sn, In, Cd, and Ga, by simply evaporating the desired commercial metal oxide powders at high temperatures. The as-synthesized oxide nanobelts are pure, structurally uniform, single-crystalline, and mostly free from dislocations; they have a rectangular-like cross-section with constant dimensions. The belt-like morphology appears to be a unique and common structural characteristic of this family of semiconducting oxides with cations of different valence states and materials of distinct crystallographic structures. Field-effect transistors[2], ultrasensitive nano-sized gas sensors[3], nanoresonators[4], and nanocantilevers[5] have been fabricated based on individual nanobelts. Thermal transport along the nanobelt has also been measured[6]. Very recently, nanobelts, nanosprings[7], and nanorings[8] that exhibit piezoelectric properties have been synthesized, which could be candidates for nanoscale transducers, actuators, and sensors.

ISSN:1369 7021 © Elsevier Ltd 2004

Among the functional oxides with perovskite, rutile, CaF_2, spinel, and wurtzite structures[9], ZnO is unique because it exhibits dual semiconducting and piezoelectric properties. ZnO is a material that has diverse structures, whose configurations are much richer than any known nanomaterials including carbon nanotubes. Using a solid-state thermal sublimation process and controlling the growth kinetics, local growth temperature, and the chemical composition of the source materials, a wide range of nanostructures of ZnO have been synthesized (Fig. 1). This review focuses on the formation of nanohelixes, nanobows, nanopropellers, nanowires, and nanocages of ZnO.

Nanohelixes/nanosprings and seamless nanorings

The wurtzite structure family has a few important members, such as ZnO, GaN, AlN, ZnS, and CdSe, which are important materials for applications in optoelectronics, lasing, and piezoelectricity. The two important characteristics of the wurtzite structure are the noncentral symmetry and polar surfaces. The structure of ZnO, for example, can be described as a number of alternating planes composed of tetrahedrally coordinated O^{2-} and Zn^{2+} ions, stacked alternately along the *c*-axis (Fig. 2a). The oppositely charged ions produce positively charged (0001)-Zn and negatively charged $(000\bar{1})$-O polar surfaces, resulting in a normal dipole moment and spontaneous polarization along the *c*-axis, as well as a divergence in surface energy.

By adjusting the raw materials with the introduction of impurities, such as In, we have synthesized a nanoring structure of ZnO (Fig. 2)[8]. High-magnification scanning electron microscopy (SEM) images clearly show the perfect circular shape of the complete ring, with uniform shape and flat surfaces. Transmission electron microscopy (TEM) images

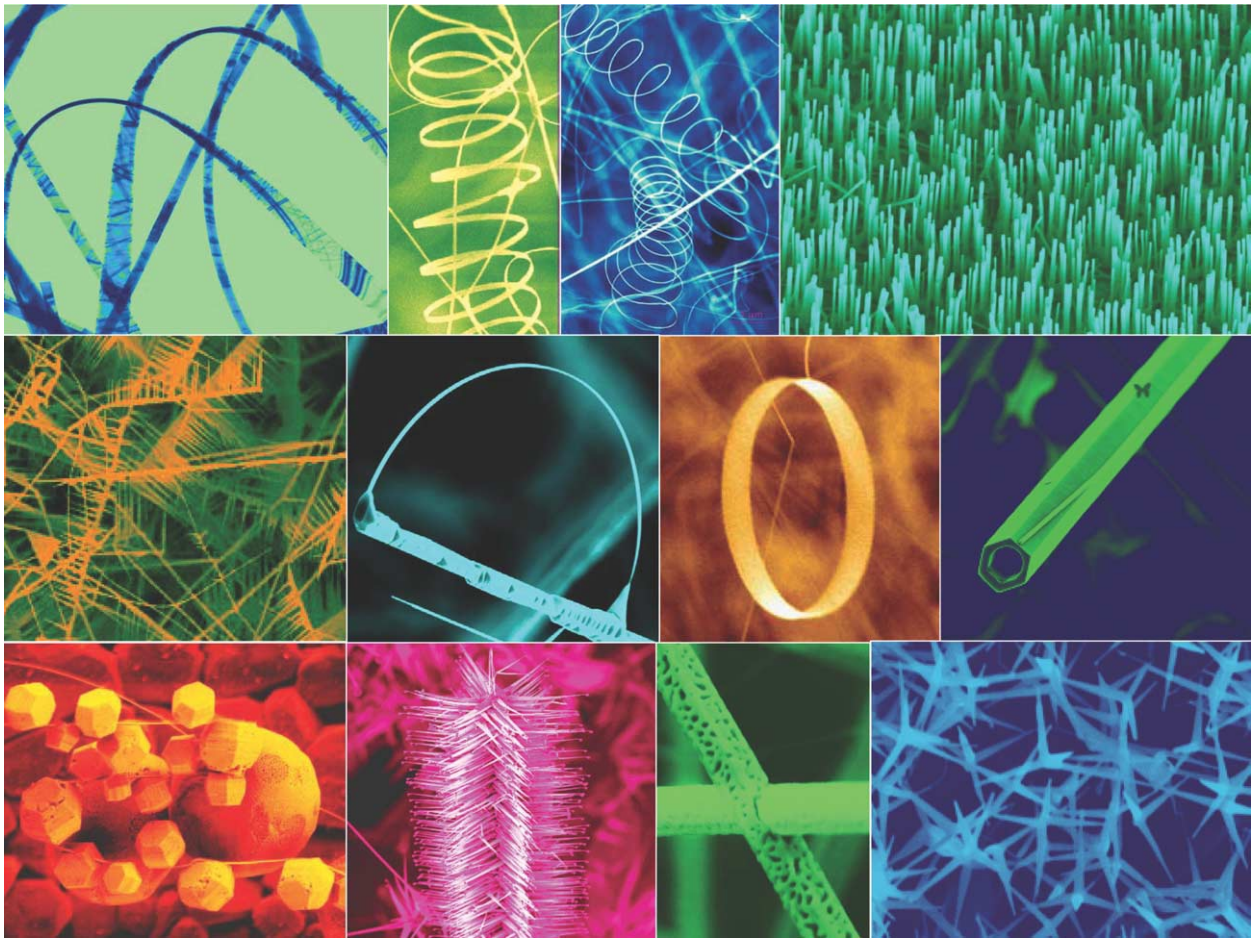

Fig. 1 A collection of nanostructures of ZnO synthesized under controlled conditions by thermal evaporation of solid powders. Most of the structures presented can be produced with 100% purity.

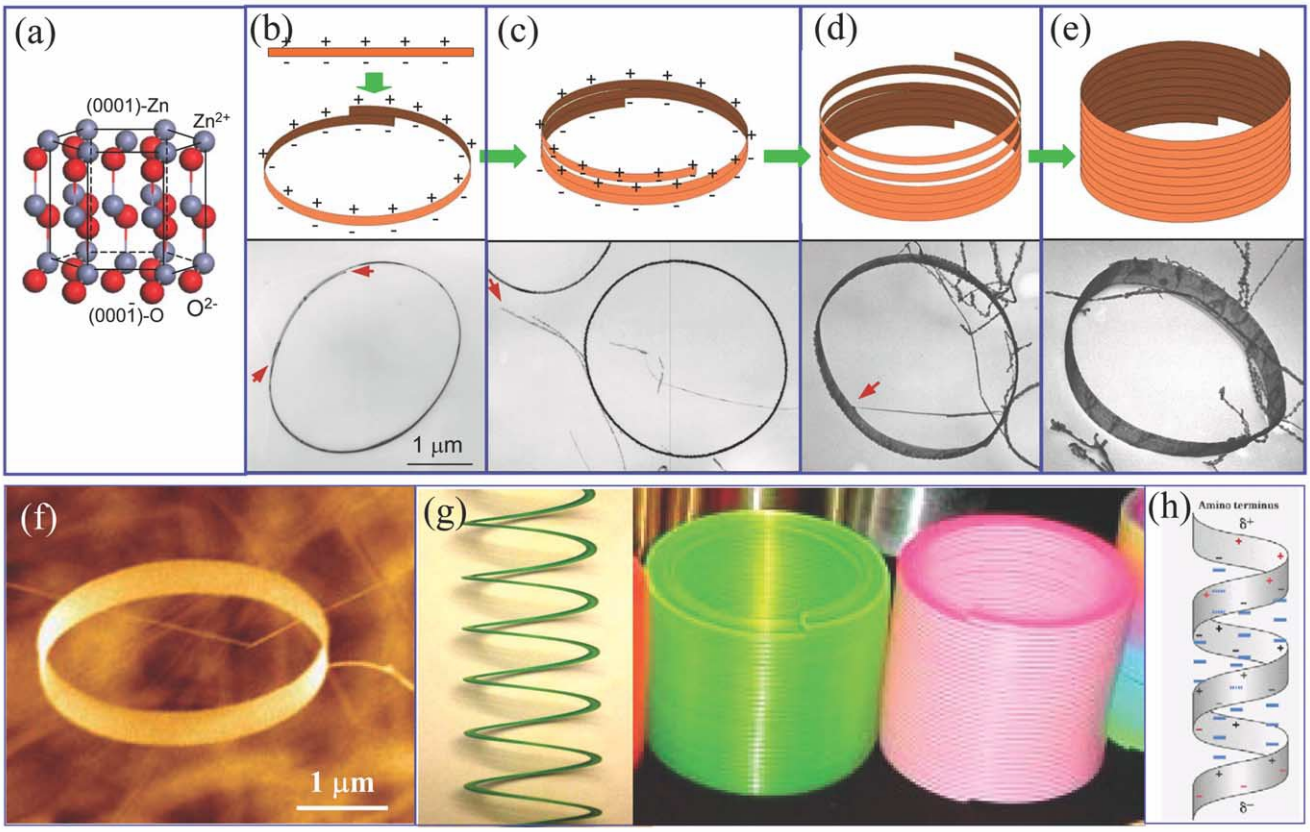

Fig. 2 Seamless single-crystal nanorings of ZnO. (a) Structure model of ZnO, showing the ±(0001) polar surfaces. (b-e) Proposed growth process and corresponding experimental results showing the initiation and formation of the single-crystal nanoring via the self-coiling of a polar nanobelt. The nanoring is initiated by folding a nanobelt into a loop with overlapped ends as a result of long-range electrostatic interactions among the polar charges; the short-range chemical bonding stabilizes the coiled ring structure; and the spontaneous self-coiling of the nanobelt is driven by minimization of the energy contributed by polar charges, surface area, and elastic deformation. (f) SEM images of the as-synthesized, single-crystal ZnO nanoring. (g) The 'slinky' growth model of the nanoring. (h) The charge model of an α-helix protein, in analogy to the charge model of the nanobelt during the self-coiling process.

indicate that the nanoring is a single-crystal entity with a circular shape. The single-crystal structure referred to here means a complete nanoring made of a single-crystalline ribbon bent evenly at the curvature of the nanoring. The nanoring is the result of coaxial, uniradius, epitaxial coiling of a nanobelt.

The growth of nanoring structures can be understood by considering the polar surfaces of the ZnO nanobelt. The polar nanobelt, which is the building block of the nanoring, grows along $[10\bar{1}0]$, with side surfaces $\pm(1\bar{2}10)$ and top/bottom surfaces ±(0001), and has a typical width of ~15 nm and thickness of ~10 nm. The nanobelt has polar charges on its top and bottom surfaces (Fig. 2b). If the surface charges are uncompensated during growth, the nanobelt may tend to fold itself, as it lengthens, to minimize the area of the polar surface. One possible way is to interface the positively charged (0001)-Zn plane (top surface) with the negatively charged $(000\bar{1})$-O plane (bottom surface), resulting in neutralization of the local polar charges and reduction of the surface area, thus forming a loop with an overlapped end (Fig. 2b). The radius of the loop may be determined by the initial folding of the nanobelt during early growth, but the size of the loop cannot be too small to reduce the elastic deformation energy. The total energy involved in the process comes from the polar charges, surface area, and elastic deformation. The long-range electrostatic interaction is likely to be the initial driving force for the folding of the nanobelt to form the first loop for subsequent growth. As the growth continues, the nanobelt may be naturally attracted onto the rim of the nanoring because of electrostatic interactions and may extend parallel to the rim of the nanoring to neutralize the local polar charge and reduce the surface area. This results in the formation of a self-coiled, coaxial, uniradius, multilooped nanoring structure (Fig. 2c). The self-assembly is spontaneous, which means that the self-coiling along the rim proceeds as the nanobelt grows. The reduced surface area

and the formation of chemical bonds (short-range forces) between the loops stabilize the coiled structure. The width of the nanoring increases as more loops wind along the nanoring axis, and all remain in the same crystal orientation (Fig. 2d). Since the growth is carried out in a temperature region of 200-400°C, 'epitaxial sintering' of the adjacent loops forms a single-crystal cylindrical nanoring structure, and the loops of the nanobelt are joined by chemical bonds into a single entity (Fig. 2e). A uniradius, perfectly aligned coiling is energetically favorable because of the complete neutralization of the local polar charges inside the nanoring (Fig. 2f) and the reduced surface area. This is the 'slinky' growth model of the nanoring shown in Fig. 2g. The charge model of the nanoring is analogous to the α-helix protein molecule (Fig. 2h).

We have recently synthesized ZnO nanobelts that are dominated by the (0001) polar surface[7]. The nanobelt grows along $[2\bar{1}\bar{1}0]$ (the *a*-axis), with its top/bottom surfaces ±(0001) and the side surfaces ± $(01\bar{1}0)$. Because of their thinness (5-20 nm) and large aspect ratio (~1:4), the flexibility and toughness of the nanobelts is extremely high. A polar-surface-dominated nanobelt can be approximated to be a capacitor with two parallel charged plates (Fig. 3a). The polar nanobelt tends to roll over into an enclosed ring to reduce the electrostatic energy (Fig. 3b). A spiral shape can also reduce the electrostatic energy (Fig. 3c). The formation of the nanorings and nanohelixes can be understood from the nature of the polar surfaces. If the surface charges are uncompensated during the growth, the spontaneous polarization induces electrostatic energy as a result of the dipole moment. But rolling up to form a circular ring would minimize or neutralize the overall dipole moment, reducing the electrostatic energy. On the other hand, bending the nanobelt produces elastic energy. The stable shape of the nanobelt is determined by the minimization of the total energy contributed by spontaneous polarization and elasticity.

If the nanobelt is rolled uniradially loop-by-loop, the repulsive force between the charged surfaces stretches the nanohelix, while the elastic deformation force pulls the loops together; the balance between the two forms the nanohelix/nanospring shown in Fig. 3d. The nanohelix has a uniform shape with a radius of ~500-800 nm and evenly distributed pitches. Each is made of a uniformly deformed single-crystal ZnO nanobelt.

The striking new feature of the nanorings and nanohelixes of single-crystalline ZnO nanobelts reported here is that they are spontaneous-polarization-induced structures, the result of

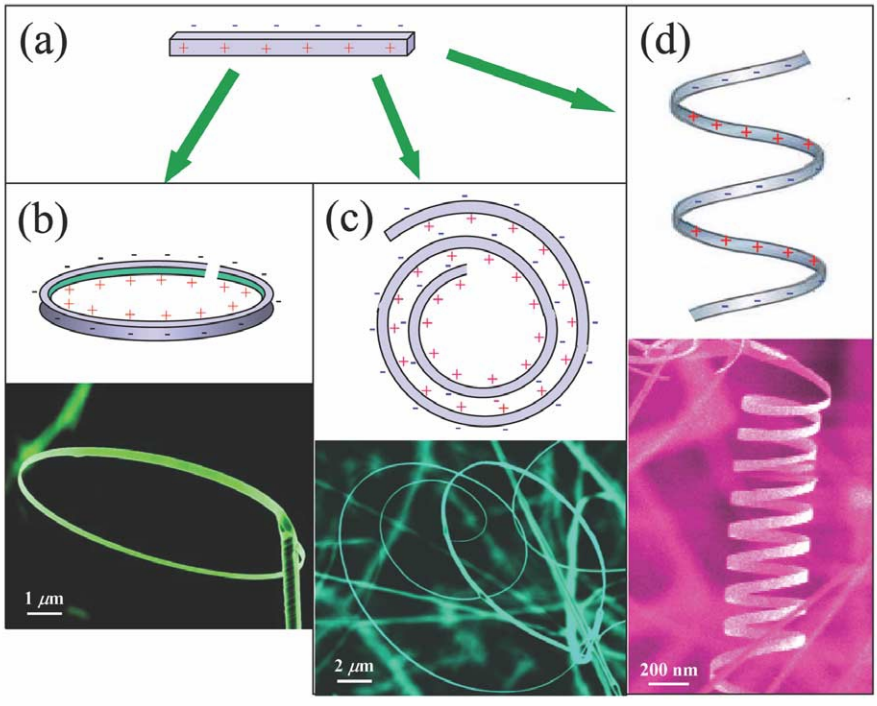

Fig. 3 (a) Model of a polar nanobelt. Polar-surface-induced formation of (b) nanorings, (c) nanospirals, and (d) nanohelixes of ZnO and their formation processes.

a 90° rotation in polarization. These are ideal objects for understanding piezoelectricity and polarization-induced phenomena at the nanoscale. The piezoelectric nanobelt structures could also be used as nanoscale sensors, transducers, or resonators.

Aligned nanopropellers

Modifying the composition of the source materials can drastically change the morphology of the grown oxide nanostructure. We used a mixture of ZnO and SnO_2 powders in a weight ratio of 1:1 as the source material to grow a complex ZnO nanostructure[10,11]. Fig. 4a is an SEM image of the as-synthesized products showing a uniform feature consisting of sets of central axial nanowires, surrounded by radially oriented 'tadpole-like' nanostructures. The morphology of the string appears like a 'liana', while the axial nanowire is like 'rattan', which has a uniform cross-section with dimensions in the range of a few tens of nanometers. The tadpole-like branches have spherical balls at the tips (Fig. 4a), and the branches display a ribbon shape. The ribbon branches have a fairly uniform thickness, and their surfaces are rough with steps. Secondary growth on the 'propeller' surface leads to aligned nanowires (Fig. 4b).

It is known that SnO_2 can decompose into Sn and O_2 at high temperature, thus the growth of the nanowire-nanoribbon junction arrays is the result of the vapor-liquid-solid (VLS) growth process, in which Sn catalyst particles are responsible for initiating and leading the growth of ZnO nanowires and nanoribbons. The growth of the novel structures presented here can be separated into two stages. The first stage is fast growth of the ZnO axial nanowire along [0001] (Fig. 4c). The growth rate is so high that a slow increase in the size of the Sn droplet has little influence on the diameter of the nanowire, thus the axial nanowire has a fairly uniform shape along the growth direction. The second stage is the nucleation and epitaxial growth of nanoribbons as a result of the arrival of tiny Sn droplets onto the ZnO nanowire surface (Fig. 4d). This stage is much slower than the first one because the lengths of the nanoribbons are uniform and much shorter than that of the nanowire. Since Sn is in a liquid state at the growth temperature, it tends to adsorb the newly arriving Sn species and grows into a larger size particle (i.e. coalesces). Therefore, the width of the nanoribbon increases as the size of the Sn particle at the tip becomes larger, resulting in the formation of the tadpole-like structure

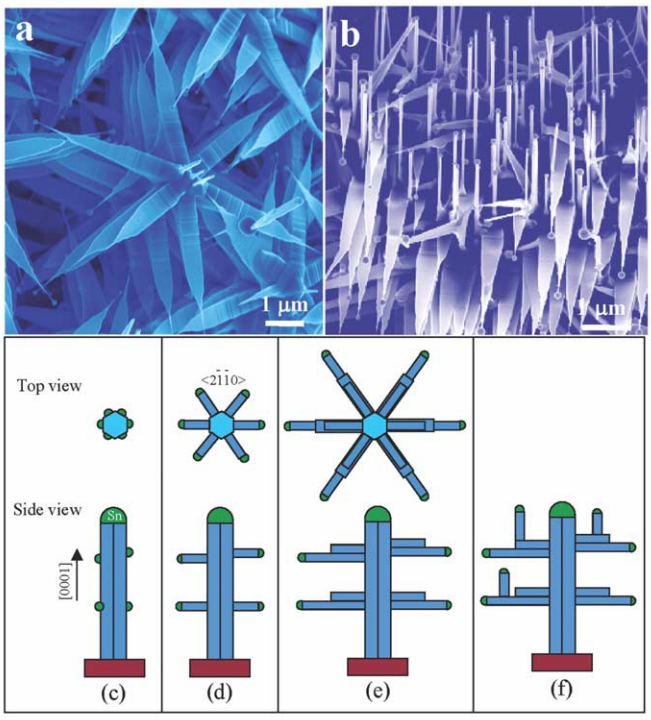

Fig. 4 Nanopropeller arrays of ZnO. (a) SEM image of Sn-catalyzed growth of aligned nanopropellers based on the six equivalent crystallographic directions. (b) Secondary growth of nanowires on the surface of the nanopropellers. (c-f) Growth process of the nanopropellers.

observed in the TEM (Fig. 4e). The Sn liquid droplets deposited onto the ZnO nanowire lead to the simultaneous growth of ZnO nanoribbons along six equivalent growth directions: ±[10$\bar{1}$0], ±[0$\bar{1}$10], and ±[$\bar{1}$100]. Secondary growth along [0001] results in the growth of aligned nanowires on the surfaces of the propellers (Fig. 4f).

Patterned growth of aligned nanowires

The growth of patterned and aligned one-dimensional nanostructures is important for applications in sensing[2,3], optoelectronics, and field emission[12,13]. Aligned growth of ZnO nanorods has been successfully achieved on a solid substrate via the VLS process with the use of Au[14,15] and Sn[16] as catalysts, which initiate and guide the growth. The epitaxial orientation relationship between the nanorods and the substrate leads to aligned growth. Other techniques that do not use catalysts, such as metalorganic vapor-phase epitaxial growth[17], template-assisted growth[12], and electrical field alignment[18] have also been employed for the growth of vertically aligned ZnO nanorods. Huang *et al.* have demonstrated a technique for growing periodically arranged carbon nanotubes using a catalyst pattern produced from a

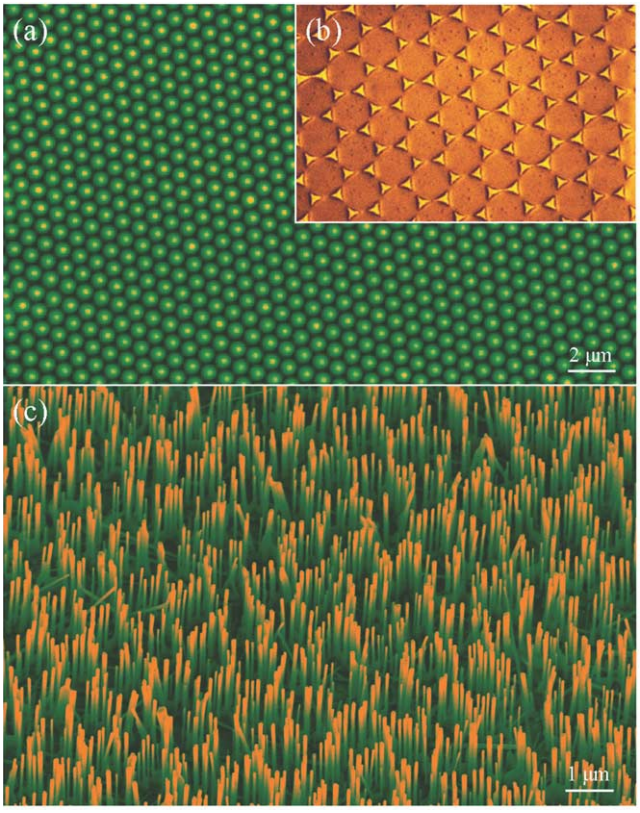

Fig. 5 Growth of patterned and aligned ZnO nanowires. (a) Self-assembled monolayer of polystyrene spheres that serves as a mask. (b) Hexagonally patterned Au catalyst on the substrate. (c) Aligned ZnO nanowires grown on a single-crystal alumina substrate in a honeycomb pattern defined by the catalyst mask.

mask and self-assembled submicron spheres[19]. We have combined this self-assembly-based mask technique with the surface epitaxial approach to grow large-area hexagonal arrays of aligned ZnO nanorods[20].

The synthesis process involves three main steps. The hexagonally patterned ZnO nanorod arrays are grown on a single-crystal Al_2O_3 substrate on which patterned Au catalyst particles have been dispersed. First, a two-dimensional, large-area, self-assembled and ordered monolayer of submicron polystyrene spheres is introduced onto the single-crystal Al_2O_3 substrate (Fig. 5a). Second, a thin layer of Au particles is deposited onto the self-assembled monolayer; the spheres are then etched away, leaving a patterned Au catalyst array (Fig. 5b). Finally, nanowires are grown on the substrate using the VLS process (Fig. 5c). The spatial distribution of the catalyst particles determines the pattern of the nanowires. This step can be achieved using a variety of mask technologies for producing complex configurations. By choosing the optimum match between the substrate lattice and the nanowires, the epitaxial orientation relationship between the nanowire and the substrate results in the aligned growth of nanowires normal to the substrate. The distribution of the catalyst particles defines the location of the nanowires, and the epitaxial growth on the substrate results in the vertical alignment.

Mesoporous single-crystal nanowires

Porous materials have a wide variety of applications in bioengineering, catalysis, environmental engineering, and sensor systems because of their high surface-to-volume ratio. Normally, most of these mesoporous structures are composed of amorphous materials and porosity is achieved by solvent-based organic or inorganic reactions. There are few reports of mesoporous structures based on crystalline material.

We have reported a novel wurtzite ZnO nanowire structure that is a single crystal but is composed of mesoporous walls/volumes[21]. The synthesis is based on a modified solid-vapor process. Fig. 6a shows an SEM image of the as-synthesized ZnO nanowires grown on a Si substrate coated with a thin layer of Sn catalyst. The typical length of the nanowires varies from 100 μm to 1 mm and the diameter

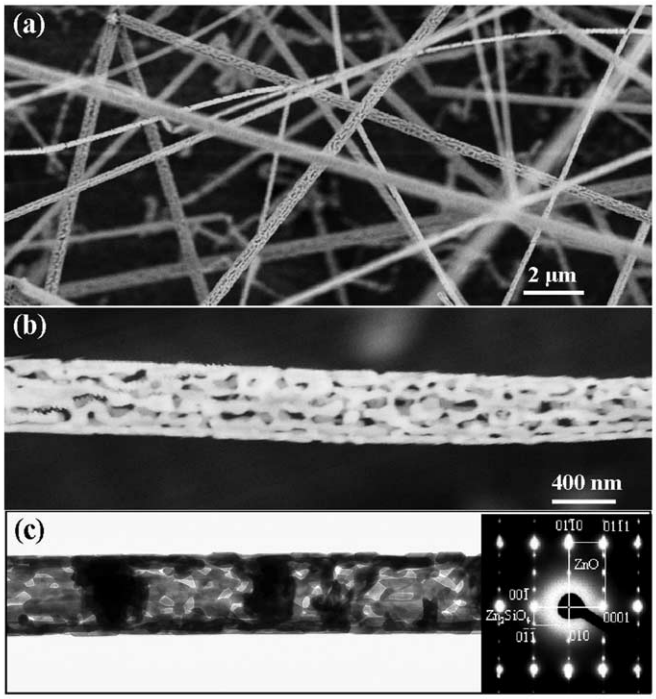

Fig. 6 Mesoporous, single-crystal ZnO nanowires. (a) SEM image of high-porosity ZnO nanowires grown on an Sn-coated Si substrate. (b) High-magnification SEM images showing the morphology of a single nanowire. (c) Low-magnification TEM image of a porous ZnO nanowire and corresponding electron diffraction pattern, showing that the ZnO porous wire is covered by a thin layer of Zn_2SiO_4.

is in the range of 50-500 nm. The porous structure of the ZnO nanowires is apparent (Fig. 6b). A corresponding electron diffraction pattern from the nanowire presents two sets of structures (Fig. 6c): the brighter spots are the $[2\bar{1}\bar{1}0]$ zone axis pattern, and the nanowire axial direction is [0001]; the weaker diffraction spots, together with the chemical composition provided by energy dispersive X-ray spectroscopy (EDS), show the formation of Zn_2SiO_4 on the surface of the nanowires with an epitaxial orientation relationship as follows,
$(0001)_{ZnO} \parallel (001)_{Zn_2SiO_4}$, $[2\bar{1}\bar{1}0]_{ZnO} \parallel [100]_{Zn_2SiO_4}$.
Zn_2SiO_4 is formed on the surface of the Si substrate, but covers only a fraction of the surface area because of the large lattice mismatch with ZnO. As a result, resublimation of ZnO in the nanowire forms the mesoporous structure[21]. The high-porosity, single-crystal wire-like structures have potential applications as filters, catalyst supports, and gas sensors.

Ultra-narrow ZnO nanobelts

To investigate quantum confinement effects, nanobelts of small sizes are required. We have recently grown ultra-small nanobelts with the VLS growth method using a novel catalyst[22]. Instead of using dispersive nanoparticles as the catalyst for seeded growth, a uniform thin film (~10 nm) of Sn was coated onto the Si substrate. The ZnO nanobelts produced by the Sn film catalyst are rather narrow, thin, and uniform (Fig. 7a). Electron diffraction patterns and high-resolution TEM images show that the nanobelts grow along [0001], their top surfaces are $(2\bar{1}\bar{1}0)$ and their side surfaces are $(0\bar{1}10)$. The average diameter of the nanobelts is 5.5 nm with a standard deviation of ±1.5 nm, indicating a very good size uniformity.

To examine size-induced quantum effects in the ultrathin ZnO nanobelts, photoluminescence (PL) measurements were performed at room temperature using an Xe lamp with an excitation wavelength of 330 nm (Fig. 7b). In comparison with the PL measurements from nanobelts with an average width of ~200 nm, the 6 nm nanobelts show a 14 nm shift in the emission peak, which possibly indicates quantum confinement arising from the reduced size of the nanobelts.

Polyhedral cages

Cages of ZnO have also been synthesized at a high yield and purity[23]. The mesoporous-structured polyhedral drum and spherical cages and shells are formed by textured self-assembly of ZnO nanocrystals, which are made by a novel self-assembly process during epitaxial surface oxidation (Fig. 8) The cages and shells exhibit unique geometrical shapes and their walls are composed of mesoporous, textured ZnO nanocrystals. The structures of the cages and shells are being studied and a growth mechanism has been proposed that comprises a process following solidification of the Zn liquid droplets, surface oxidation, and sublimation. This is a new approach to the synthesis of self-assembled nanostructures. The textured cage and shell structures reported here could be useful for drug delivery.

Outlook

ZnO is a typical member of the wurtzite family of structures. As a result of the three fastest growth directions, <0001>, $<01\bar{1}0>$, and $<2\bar{1}\bar{1}0>$, and polar surface induced phenomena, a diverse group of ZnO nanostructures has been grown. It can

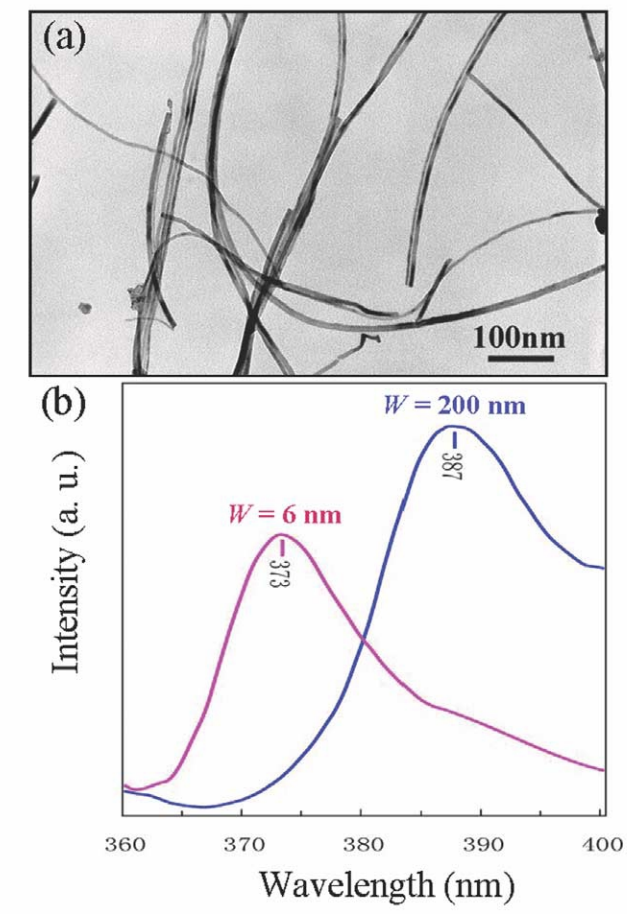

Fig. 7 Ultra-narrow ZnO nanobelts. (a) TEM image of a ZnO nanobelt grown using a Sn thin-film catalyst. (b) PL spectra of the wide (W = 200 nm) and narrow nanobelts (W = 6 nm), showing the blue shift in the emission peak as a result of size effects.

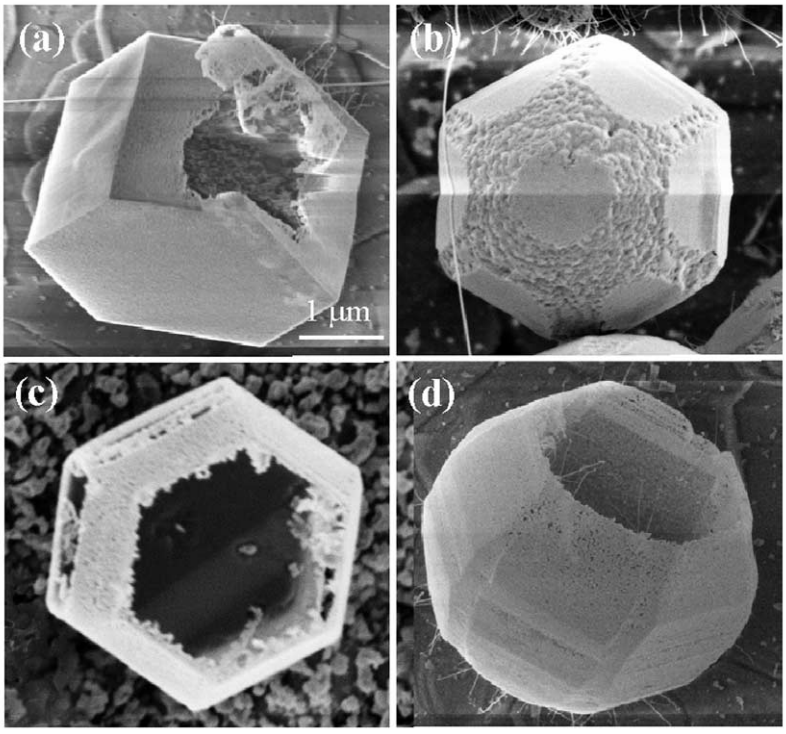

Fig. 8 Single-crystalline, polyhedral cages and shells of ZnO.

be predicted that ZnO is probably the richest family of nanostructures among all one-dimensional nanostructures, including carbon nanotubes.

ZnO has three key advantages. First, it is semiconductor, with a direct wide band gap of 3.37 eV and a large excitation binding energy (60 meV). It is an important functional oxide, exhibiting near-ultraviolet emission and transparent conductivity. Secondly, because of its noncentral symmetry, ZnO is piezoelectric, which is a key property in building electromechanical coupled sensors and transducers. Finally, ZnO is bio-safe and biocompatible, and can be used for biomedical applications without coating. With these three unique characteristics, ZnO could be one of the most important nanomaterials in future research and applications. The diversity of nanostructures presented here for ZnO should open up many fields of research in nanotechnology. MT

Acknowledgments

Thanks to Y. Ding, P. X. Gao, W. L. Hughes, X. Y. Kong, C. Ma, D. Moore, Z. W. Pan, C. J. Summers, X. D. Wang, and Y. Zhang for helpful discussion and their contributions to the work reviewed in this article. We acknowledge generous support by the Defense Advanced Projects Research Agency, National Science Foundation, and NASA.

REFERENCES

1. Pan, Z. W., *et al., Science* (2001) **291**, 1947
2. Arnold, M. S., *et al., J. Phys. Chem. B* (2003) **107** (3), 659
3. Comini, E., *et al., Appl. Phys. Lett.* (2002) **81** (10), 1869
4. Bai, X. D., *et al., Appl. Phys. Lett.* (2003) **82** (26), 4806
5. Hughes, W. L., and Wang, Z. L., *Appl. Phys. Lett.* (2003) **82** (17), 2886
6. Shi, L., *et al., Appl. Phys. Lett.* (2004) **84** (14), 2638
7. Kong, X. Y., and Wang, Z. L., *Nano Lett.* (2003) **3** (12), 1625
8. Kong, X. Y., *et al., Science* (2004) **303**, 1348
9. Wang, Z. L., and Kang, Z. C., *Functional and Smart Materials – Structural Evolution and Structure Analysis*, Plenum Press, New York, (1998)
10. Gao, P. X., and Wang, Z. L., *J. Phys. Chem. B* (2002) **106** (49), 12653
11. Gao, P. X., and Wang, Z. L., *Appl. Phys. Lett.* (2004) **84** (15), 2883
12. Liu, C., *et al., Adv. Mater.* (2003) **15** (10), 838
13. Bai, X. D., *et al., Nano Lett.* (2003) **3** (8), 1147
14. Yang, P. D., *et al., Adv. Funct. Mater.* (2002) **12** (5), 323
15. Zhao, Q. X., *et al., Appl. Phys. Lett.* (2003) **83** (1), 165
16. Gao, P. X., *et al., Nano Lett.* (2003) **3** (9), 1315
17. Park, W. I., *et al., Appl. Phys. Lett.* (2002) **80** (22), 4232
18. Harnack, O., *et al., Nano Lett.* (2003) **3** (8), 1097
19. Huang, Z. P., *et al., Appl. Phys. Lett.* (2003) **82** (3), 460
20. Wang, X. D., *et al., Nano Lett.* (2004) **4** (3), 423
21. Wang, X. D., *et al., Adv. Mater.* (2004), in press
22. Wang, X. D., *et al., J. Phys. Chem. B* (2004), in press
23. Gao, P. X., and Wang, Z. L., *J. Am. Chem. Soc.* (2003) **125** (37), 11299